Two synaptobrevin molecules are sufficient for vesicle fusion in central nervous system synapses

Raunak Sinha[a,b], Saheeb Ahmed[c], Reinhard Jahn[c], and Jurgen Klingauf[a,b,1]

Departments of [a]Membrane Biophysics and [c]Neurobiology, Max-Planck Institute for Biophysical Chemistry, 37077 Göttingen, Germany; and [b]Department of Cellular Biophysics, Institute for Medical Physics and Biophysics, University of Muenster, 48149 Muenster, Germany

Edited by Thomas C. Südhof, Stanford University School of Medicine, Palo Alto, CA, and approved July 14, 2011 (received for review February 2, 2011)

Exocytosis of synaptic vesicles (SVs) during fast synaptic transmission is mediated by soluble *N*-ethylmaleimide-sensitive factor attachment protein receptor (SNARE) complex assembly formed by the coil-coiling of three members of this protein family: vesicle SNARE protein, synaptobrevin 2 (syb2), and the presynaptic membrane SNAREs syntaxin-1A and SNAP-25. However, it is controversially debated how many SNARE complexes are minimally needed for SV priming and fusion. To quantify this effective number, we measured the fluorescence responses from single fusing vesicles expressing pHluorin (pHl), a pH-sensitive variant of GFP, fused to the luminal domain of the vesicular SNARE syb2 (spH) in cultured hippocampal neurons lacking endogenous syb2. Fluorescence responses were quantal, with the unitary signals precisely corresponding to single pHluorin molecules. Using this approach we found that two copies of spH per SV fully rescued evoked fusion whereas SVs expressing only one spH were unable to rapidly fuse upon stimulation. Thus, two syb2 molecules and likely two SNARE complexes are necessary and sufficient for SV fusion during fast synaptic transmission.

synaptopHluorin | membrane fusion | single molecule bleaching | SNARE density

In conventional neuronal synapses, fast synaptic transmission is mediated by release of neurotransmitter upon Ca^{2+}-triggered synaptic vesicle (SV) exocytosis. This process is exquisitely regulated both spatially and temporally. The core of the SV fusion machinery is formed by three members of the soluble *N*-ethylmaleimide-sensitive factor attachment protein receptor (SNARE) protein family, which is characterized by conserved sequences of 60–70 amino acids called SNARE motifs: vesicle SNARE protein, synaptobrevin-2 (syb2), and the presynaptic membrane SNAREs syntaxin-1A and SNAP-25 (1–3).

Zipper-like assembly of the SNARE motifs from their N-terminal ends toward their membrane-proximal C termini results in the formation of a highly stable heterotrimeric "trans-SNARE complex" (also called "SNAREpin"), consisting of four parallel α-helices, which brings the two membranes into close apposition for fusion (4–7). Previous studies have suggested that several of these SNARE complexes might assemble in rosette-shaped multivalent supercomplexes, forming a ring, around the fusion pore; however, there is no direct evidence in support of this model (5, 8, 9). Therefore, the precise number of SNARE complexes minimally required to drive membrane fusion is highly debated and current estimates range between 1 and 15 (10–18). Some of these results are based on single-molecule fluorescence measurements in artificially reconstituted liposomes, whereas others are based on theoretical models, kinetic analysis, and extrapolations from dose–response relationships. Therefore, it is essential to apply a more direct method capable of visualizing single SNARE complexes in real time in a physiological setting.

In the present study we have used a unique direct approach to count the number of syb2 molecules required for fast Ca^{2+}-triggered exocytosis in living hippocampal neurons. To quantify the effective number of syb2 molecules, we measured the fluorescence responses from single fusing vesicles expressing synaptopHluorin (spH) (19) on a genetic null background and calibrated the fluorescence signals to those of single pHluorin (pHl) molecule fluorescence measured in vitro.

Results

Single-Vesicle Fusion Events Reveal Quantal Incorporation of Single-Molecule pHluorin-Tagged Proteins into Synaptic Vesicles upon Transient Overexpression. When pHl is fused to the luminal domain of SV proteins, its fluorescence is quenched at the acidic intravesicular pH of ∼5.5, but its fluorescence increases ∼25-fold when exposed to the neutral extracellular pH during exocytosis (19). The resolution of such measurements is primarily limited by background fluorescence caused by a fraction of pHl-tagged SV proteins that are localized to the presynaptic membrane under resting conditions. Although this surface fraction is small for the pHl-tagged vesicle glutamate transporter 1 (vGlut-pHl) and synaptophysin 1 (syp-pHl) with ∼2–3% for vGlut-pHl (20) and ∼9% for syp-pHl (21), it is very high for pHl-tagged syb2 (spH) with up to 25% (20, 22, 23). Thus, single vesicle fusion events can be easily visualized using vGlut-pHl (20) or syp-pHl (21) as reporters (Fig. S1), but only one study reported single vesicle resolution following viral overexpression of spH (22), the protein of interest here. This spH background fluorescence, however, can be selectively attenuated by photobleaching because the quenched intravesicular spH is largely protected against bleaching (22). If bleaching is executed rapidly (relative to spontaneous SV fusion and recycling), the resident surface pool is mostly bleached whereas exo- and endocytic trafficking of spH remains unaffected (Fig. S2) (23). Indeed, prebleaching for 50 s allowed for resolving single SV fusion events in synaptic boutons of spH-expressing wild-type (WT) hippocampal neurons in culture, when stimulated by single action potentials (AP) (Fig. 1*A*). SpH fluorescence responses from individual boutons exhibited instantaneous increases upon stimulation (Fig. 1 *A* and *B*), indistinguishable from responses obtained from boutons expressing either syp-pHl or vGlut-pHl (Fig. S1). The distributions of fluorescence intensity changes ΔF for all three reporters displayed several equidistant peaks (Fig. 1*C* and Fig. S1). The zero-order peak represents failures to evoke fusion, whereas the higher-order peaks represent release of one, two, or more packages (quanta) of pHl molecules. These quanta may originate from the fusion of single SVs (20–22) or alternatively from multiple, simultaneously fusing SVs with a varying number of pHl molecules. To quantify the quantal size q, the fluorescence contribution of a single fusing SV, we fitted the histograms to multiple Gaussian curves (24, 25) (*Materials and Methods*) yielding very similar values for the reporters, namely 14.7 ± 0.08 arbitrary units (a.u.) for syp-pHl, 14.7 ± 0.15 a.u. for vGlut-pHl, and 15.2 ± 0.21 a.u. for spH (Fig. 1*C* and Fig. S1).

To calibrate the quantal sizes in terms of numbers of pHl-tagged proteins per SV we imaged isolated pHl molecules immobilized on a coverslip (26) (Fig. 1*D*). Single pHl molecules were identified by photobleaching in single steps (Fig. 1*E*). The distribution of fluorescence downsteps at pH 9 was well de-

Author contributions: R.S. and J.K. designed research; R.S. and S.A. performed research; R.S. and J.K. analyzed data; and R.S., R.J., and J.K. wrote the paper.

The authors declare no conflict of interest.

This article is a PNAS Direct Submission.

[1]To whom correspondence should be addressed. E-mail: klingauf@uni-muenster.de.

This article contains supporting information online at www.pnas.org/lookup/suppl/doi:10.1073/pnas.1101818108/-/DCSupplemental.

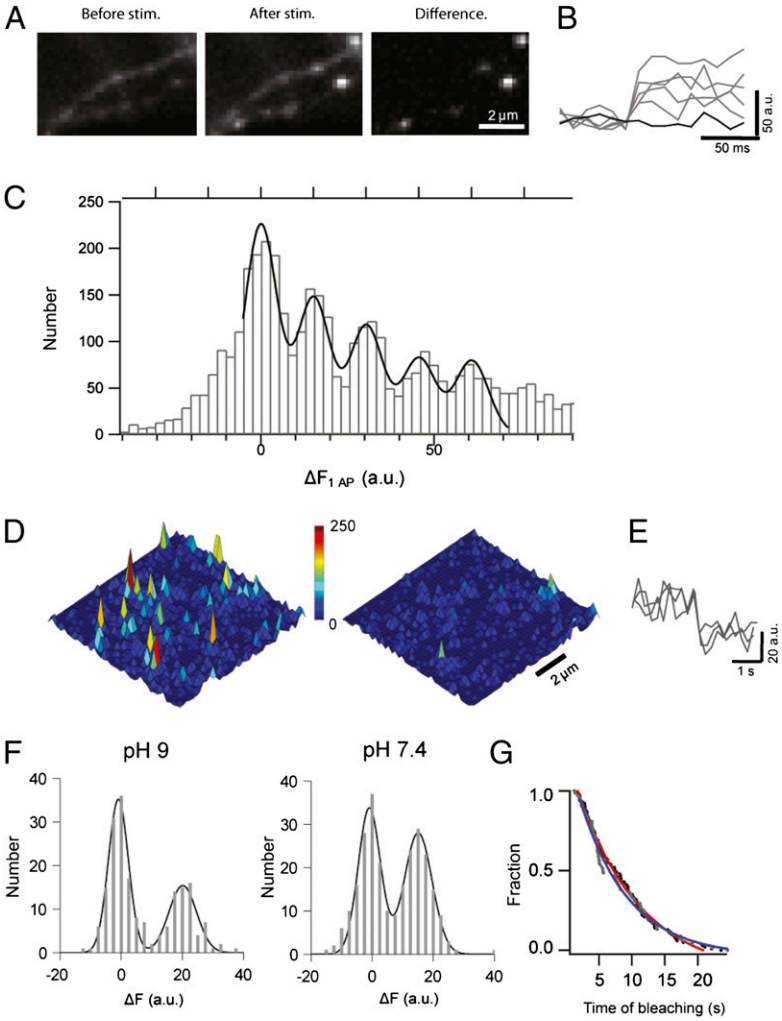

Fig. 1. Quantal size of evoked single-vesicle fluorescence response corresponds to single pHluorin molecule. (*A*) Images of spH transfected synaptic boutons before and after stimulation with 1 AP. Spots on the difference image indicate sites of triggered vesicle fusion. (*B*) Representative fluorescence profiles of evoked release. (*C*) ΔF histograms from spH transfected boutons. Bin width is 2.5 a.u. The solid line is the overall fit to multiple Gaussians of fixed quantal size $q \pm$ SD. The estimated q for spH is 15.2 ± 0.21 a.u (adjusted $R^2 = 0.94$; $n > 400$ boutons from 14 experiments). (*D*) Surface plot of purified pHl in a polyacrylamide gel before (*Left*) and after (*Right*) bleaching. (*E*) Representative intensity traces (average of 3 data points) show instantaneous single-molecule bleaching steps. (*F*) Single-molecule ΔF distribution (binned at 2.5 a.u.). Black and gray lines are the overall and individual fits to multiple Gaussians of a mean unitary size (m) of 20.11 ± 1.09 a.u. at pH 9 ($n = 195$, adjusted $R^2 = 0.94$) and 15.06 ± 0.35 a.u. at pH 7.4 ($n = 262$, adjusted $R^2 = 0.98$). (*G*) Distributions of bleaching waiting times of pHl at pH 9 (black) and 7.4 (gray) are fitted to monoexponential functions (blue, pH9; red, pH7.4) yielding time constants of 7.35 ± 0.43 s at pH 9 and 9.65 ± 0.28 s at pH 7.4.

scribed by a sum of two evenly spaced Gaussian curves with a mean size of 20.1 ± 1.09 a.u. (Fig. 1*F*). The center of the second peak corresponds to the mean fluorescence of single pHl molecules. To compare it with the neuronal measurements we repeated the experiments at physiological pH of 7.4 (Fig. 1*F*). We observed a shift in the mean size to 15.0 ± 0.35 a.u., fully consistent with the described pH dependence of the superecliptic pHl fluorescence (27). Likewise, the distributions of bleaching waiting times at pH 7.4 and 9, well described by single exponentials, reflected the same pH dependence (Fig. 1*G*). This result allowed us to estimate the fraction of vesicular pHl molecules bleached at pH 5.5 during the 50 s prebleaching to be <20%, consistent with our bulk measurements (Fig. S2).

As an additional control for documenting that individual intensity quanta correspond to single pHluorin molecules, we analyzed spontaneous bleaching steps of surface spH in hippocampal neurons, which occur randomly during the time course of our optical recordings (0.5 s at 100 Hz) (Fig. S3 and *SI Note*). The amplitude distribution of bleaching steps was well described by a Gaussian curve with a mean size of 14.1 ± 0.19 a.u. (Fig. S3), thus being very similar to the in vitro single-molecule intensity calculation (Fig. 1*F*). Therefore, measurements of bleaching steps of isolated pHl molecules as well as of spH molecules expressed in neurons provide similar and hence reliable estimates of single pHl molecule intensity.

On the basis of these calibrations, we can now conclude from the quantal fluorescence amplitude distributions during evoked exocytosis that SVs bear on average 1 pHl molecule (0.97 ± 0.02 spH, 0.99 ± 0.02 vGlut-pHl, and 0.96 ± 0.02 syp-pHl molecules). With the quantal size corresponding precisely to a single pHl molecule, the higher-order peaks in Fig. 1*C* thus indicate fusion either of single SVs with multiple pHl reporters or of multiple SVs. Overall these estimates are in good agreement with previous studies, suggesting that the number of fusion proteins per vesicle is low, close to one, irrespective of the type of promoter or the method of overexpression used (20, 22, 28).

SpH Rescues Ca^{2+}-Evoked Exocytosis in *synaptobrevin 2/cellubrevin 2* DKO Hippocampal Neurons. Whereas our experiments so far suggest that SVs contain on average only a single copy of a pHl-tagged SV protein, each SV has a large excess of up to 70 endogenous nonfluorescent syb2 (29), which may form SNARE complexes. Thus, it is not possible in this system to estimate the number of syb2 molecules required for exocytosis from measuring copy numbers of spH. To overcome this problem, we expressed spH in hippocampal neurons isolated from synaptobrevin2/cellubrevin2 double-knockout (DKO) mice, thus creating a situation in which neurons contain spH as the only syb2 variant. It was previously reported that in the DKO mice, secretion is completely abolished from adrenal chromaffin cells (30). Furthermore, deletion of syb2 alone, the predominant syb isoform in SVs, was shown to result in a 10-fold reduction of spontaneous fusion and a 100-fold decrease in fast Ca^{2+}-triggered exocytosis in hippocampal synapses (31), thus providing a clean loss-of-function background for rescue experiments. Indeed, expression of syb2 fused to fluorescent proteins at the luminal domain in KO neurons was previously shown to rescue evoked exocytosis (32, 33). Here, we first tested the ability of spH to rescue synaptic function in these hippocampal synapses (Fig.

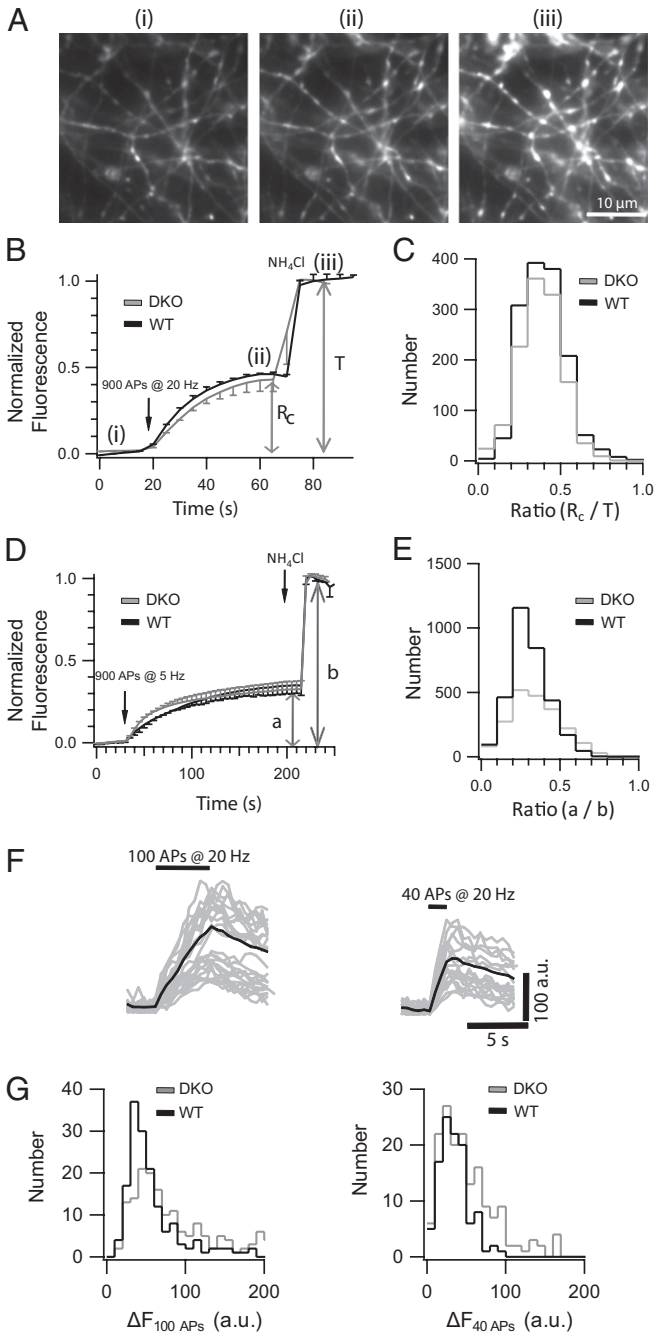

Fig. 2. SpH overexpression in syb2/ceb2 DKO hippocampal neurons rescues evoked synaptic transmission. (*A*) Fluorescence images of DKO hippocampal boutons overexpressing spH before (*i*) and after (*ii*) 900 APs stimulation and after NH_4Cl application (*iii*). (*B*) Representative average fluorescence response (DKO in gray and WT in black; $n > 300$ boutons from two experiments) to 900 APs at 20 Hz followed by NH_4Cl dequenching. R_c denotes the size of the recycling pool, i.e., the relative increase in fluorescence upon stimulation in presence of folimycin, and *T* denotes the size of the total pool, i.e., the total fluorescence increase after subsequent NH_4Cl application. (*C*) ΔF distributions of the recycling pool fraction from spH-overexpressing DKO ($n > 1{,}000$ boutons from six experiments) and WT ($n > 800$ boutons from four experiments) boutons are similar. (*D*) Average fluorescence response ($n > 300$ boutons from two experiments) to 900 APs at 5 Hz (*a*) followed by NH_4Cl dequenching (*b*). (*E*) ΔF distributions of the relative increase in fluorescence upon stimulation (*a*/*b*) from spH-overexpressing DKO ($n > 1{,}500$ boutons from seven experiments) and WT ($n > 1{,}200$ boutons from six experiments) boutons are similar. (*F*) Fluorescence responses of individual boutons to 100 APs (*Left*) and 40 APs (*Right*) at 20 Hz. The average response is overlaid (solid line). (*G*) ΔF distributions from spH-overexpressing DKO ($n > 150$ boutons from six experiments) and WT ($n > 150$ boutons from six experiments) boutons in response to 100 APs (*Left*) and 40 APs (*Right*) are similar.

2*A*). First, we compared the recycling pool size of SVs between spH-expressing WT and DKO neurons, using the alkaline trap method (34). In this procedure, the vesicular proton pump is inhibited using folimycin, which renders the SVs in an alkaline state after fusion. Thus, after mobilizing the entire recycling pool (R_c), with a train of 900 APs at 20 Hz in the presence of folimycin, the fluorescence plateaus with no recovery due to reacidification (Fig. 2 *A* and *B*). Neurons were then superfused with NH_4Cl (50 mM) after stimulation (Fig. 2 *A* and *B*), equilibrating the pH across all membranes to 7.4 and thereby unmasking any SVs that previously did not fuse. The fluorescence increase in response to the depleting stimulation relative to the total increase (T) in response to the NH_4Cl pulse yields then the fractional size of the recycling pool (R_c/T). Fluorescence responses were indistinguishable from WT (Fig. 2*B*), as well as the distribution of the recycling pool fraction. The peak of the distribution is ~0.45, which is in very good agreement with previous studies (Fig. 2*C*) (34). We repeated the above experiment with a train of 900 APs at 5 Hz, a protocol used to evoke long-term depression in hippocampal synapses, to look at SV repriming and rerelease over prolonged stimulation. Poststimulation the remaining fluorescence was dequenched with a NH_4Cl pulse. Average traces from spH overexpression in DKO boutons show no difference in kinetics and relative amplitude (Fig. 2*D*). The amplitude histograms of the fractional increase in fluorescence upon stimulation to the total increase after NH_4Cl perfectly overlaps between the DKO and WT boutons (Fig. 2*E*), indicating that spH can fully rescue evoked release in the DKO neurons, in agreement with previous patch-clamp studies of KO hippocampal neurons expressing C- and N-terminal GFP fusion constructs of syb2 (32). Furthermore fluorescence responses to trains of 40 and 100 APs, in the absence of folimycin, were indistinguishable from WT (Fig. 2*F*), as well as their amplitude distributions (Fig. 2*G*).

Two Molecules of spH Necessary and Sufficient for Evoked SV Fusion. In simple terms the above amplitude distributions reflect the product of release probability (P_r) during stimulation and the quantal content, i.e., the number of spH molecules per SV. Thus, a similar distribution might reflect either a low P_r, i.e., incomplete rescue by spH, combined with a high spH copy number per fusing SV (high quantal content), or a full rescue (same P_r) with the same low copy number of ~1 spH molecule per SV as in WT (Fig. 3*A*). The latter case would imply that SVs with only one copy of spH, i.e., capable of forming a single SNARE complex, can undergo rapid exocytosis. To distinguish between both scenarios we measured spH fluorescence responses to single AP in DKO rescue boutons. The resulting amplitude histogram looked strikingly similar to WT with peak spacing of 14.9 ± 0.28 a.u.—except for the first nonzero peak (Fig. 3*B*). Superposition of both molecular histograms revealed an almost complete lack of the first molecular peak in the DKO rescue histogram (Fig. 3*C*), suggesting that SVs with only one copy of spH are unable to fuse within milliseconds upon stimulation. We conclude that minimally two copies of spH are required to promote rapid vesicle fusion within <10 ms after stimulation, i.e., within one frame, at our 100-Hz sampling frequency.

Several controls were carried out to make sure that the actual number of syb2 molecules involved in the exocytotic events was not over- or underestimated. First, upon comparing the absolute frequencies of fusion events of SVs bearing one, two, or three spH molecules for WT and DKO rescue boutons (Fig. 4*A*), we observed a small residual one-molecule peak. This observation may suggest that SVs containing only a single spH molecule fuse occasionally. However, it cannot be excluded that during the prebleaching period a small fraction of spH inside the SV may

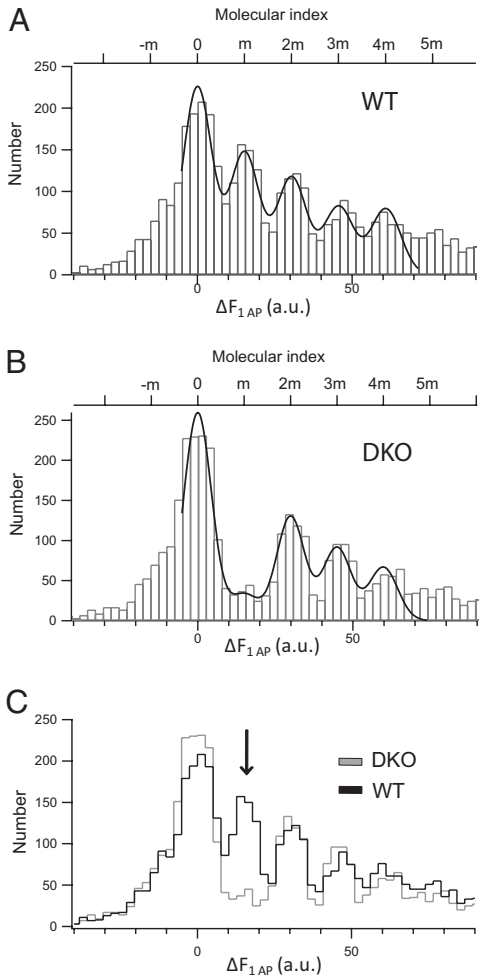

Fig. 3. SVs with a single copy of spH do not undergo Ca^{2+}-triggered exocytosis. (*A*) ΔF distribution from spH-overexpressing WT boutons plotted with bin width of 2.5 a.u. The smooth curve is the overall fit to multiple Gaussians (adjusted $R^2 = 0.94$). The estimated unitary size is 15.2 ± 0.21 a.u. ($n > 400$ boutons from 14 experiments). (*B*) ΔF distribution from spH-overexpressing DKO boutons plotted with a bin width of 2.5 a.u. The smooth curve is the overall fit to multiple Gaussians (adjusted $R^2 = 0.94$). The estimated unitary size is 14.9 ± 0.28 a.u. ($n > 400$ boutons from 15 experiments). (*C*) Superimposed intensity distributions for spH-overexpressing WT and DKO boutons. The arrow indicates the marked reduction of the first nonzero peak in spH-overexpressing DKO boutons.

become bleached despite the low pH and thus will go undetected, thus leading to an underestimation of the syb copy number. To address this issue we increased the prebleach time to 2 min (Fig. 4*B*). For quantification the amplitude ratios of the first over the second nonzero molecular peaks were calculated (Fig. 4*C*). Indeed, prolonging of the prebleaching time more than doubled this ratio for DKO, but not for WT boutons (Fig. 4*C* and Fig. S4). The ratio, however, does not significantly change during the 10 consecutive recording and bleaching periods (Fig. S5). Thus, the small first peak observed in the molecular histogram of DKO boutons is rather a consequence of prebleaching than an indication of SV fusion with only one SNARE complex. Next we tested the impact of the missing first peak on the net molecular distributions by plotting intensity-weighted histograms (Fig. S6). The distributions looked very similar with a slight but negligible (<10%) difference between WT and DKO neurons (Fig. S6). This result is consistent with the amplitude distributions from 40, 100, and 900 APs, which are indistinguishable between both WT and DKO conditions, indicating that the absence of the first peak has little or no effect on the total fluorescence change.

Underestimation may result from the expression of spH molecules that are nonfluorescent, either due to misfolding or by posttranslational proteolytic cleavage of the GFP moiety. Misfolding of GFP moieties was previously estimated to account for maximally 10–20% (35, 36), i.e., too low to account for a systematic underestimation of the number of pHluorin molecules or SNARE complexes (*SI Discussion*). To exclude cleavage of spH during trafficking to the SVs, resulting in copies of unlabeled syb2 in SVs, we performed Western blot analysis of lysates from DKO hippocampal cultures overexpressing spH, using an anti-syb2 antibody that specifically binds to the N terminus (aa 2–17) of syb2 (note that pHluorin is fused to the luminal C terminus and thus does not interfere with detection) (Fig. 4*D*). The presence of a single spH band with no cleaved syb2 product confirms that there is no significant cleavage of the fusion protein, spH, when overexpressed in the DKO background. In summary, our data provide direct evidence that two molecules of spH and thus likely two SNARE complexes are necessary and sufficient for triggered SV fusion in living central synapses.

Discussion

In this study we have resolved the minimum number of syb2 required for executing SNARE-dependent membrane fusion in functionally intact synapses. Using high-resolution fluorescence measurements of single-vesicle fusion followed by calibration with single-molecule measurements we counted the exact number of pHl-tagged vesicle proteins inserted per SV. The ΔF distributions are quantized where single pHl molecules were resolved as distinct peaks of mean size equivalent to that estimated from single pHl molecule measurements in vitro. However, when we overexpressed spH in syb2/ceb2 DKO boutons, the ΔF distributions exhibited a dramatic absence of the first molecular peak obtained from single-vesicle spH fluorescence measurements in DKO neurons, which clearly defined the lower bound of 2 syb2/spH molecules required to evoke fusion during fast synaptic transmission.

Our findings provide several insights into the process of vesicle docking, priming, and fusion during fast synaptic transmission. With a minimum of two spH molecules per SV it is difficult to imagine that SVs dock with their two SNAREs already pointing to the plasma membrane. Rather the two SV SNAREs should freely diffuse within the SV membrane and therefore should be positioned randomly on the SV surface during docking. Thus, our findings imply that initial docking is syb2 independent but rather driven by other factors such as Munc18-1 (37), syntaxin-1 (38), or, as recently shown, synaptotagmin-1 (39).

During regulated exocytosis, merger of the two membranes leads to the formation of an aqueous fusion pore whose physical properties have been long debated (40). On the basis of our results we suggest that the fusion pore is likely to be composed of lipids, two transmembrane domains of syb2, and two of syntaxin 1A (Fig. 4*E*). This suggestion implies that the inner fusion pore is predominantly lined by lipids instead of transmembrane SNARE domains arranged like barrel staves around the pore (5, 8, 9).

The finding that such a low copy number of syb2 can rescue evoked fusion raises the possibility that the kinetics of synaptic transmission, observed using spH overexpression in DKO neurons, may be slower than during normal physiological neurosecretion when there are 70 copies of syb2 present on the SV (29). However, an earlier as well as a recent study have shown that overexpression of N- or C-terminal GFP fusion constructs of syb2 in syb2-deficient hippocampal neurons fully rescues the amplitude and kinetics of evoked excitatory postsynaptic potentials in syb2-deficient neurons (32, 33).

SNARE assembly is believed to generate sufficient energy to drive membrane fusion (4, 6, 7). Recent studies using a surface force apparatus indicated that the stabilization energy of a single partially assembled neuronal SNARE complex is ~35 k_BT, which corresponds closely to the energy required for hemifusion of lipid bilayers (40–50 k_BT) (15, 41, 42). Moreover, using iso-

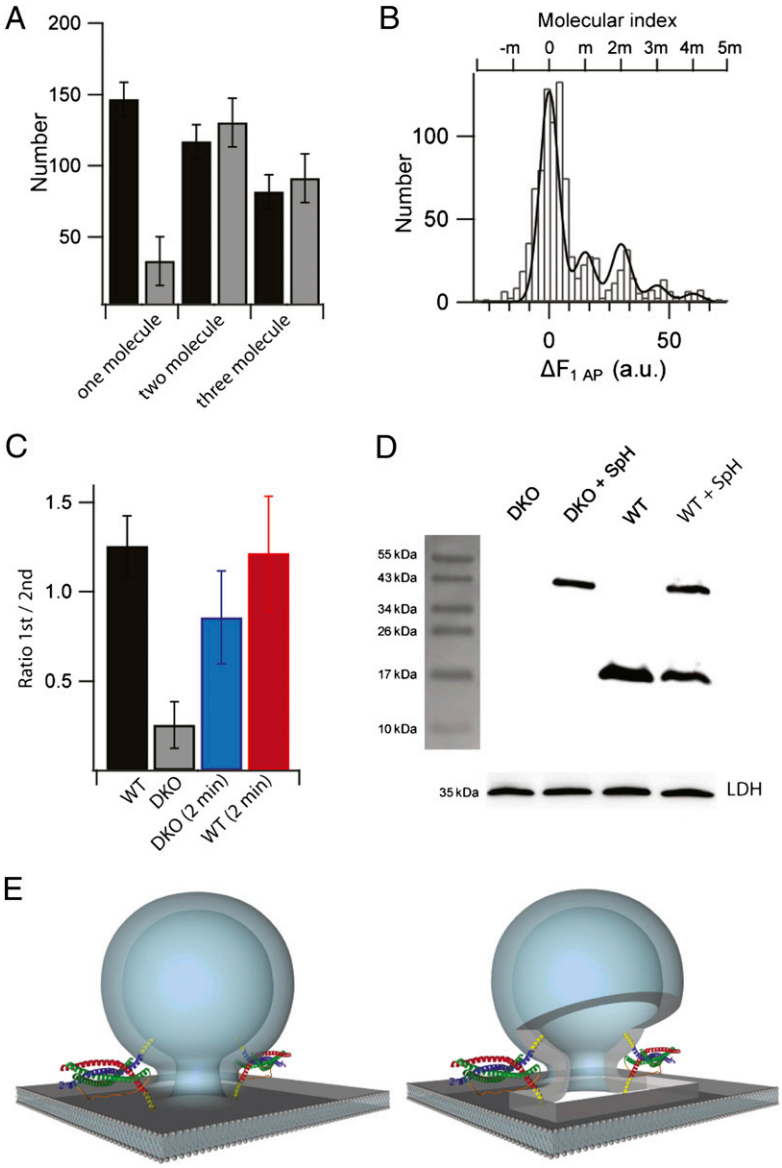

Fig. 4. Two copies of spH are minimally required to drive SV fusion. (*A*) Bar graph comparing the absolute amplitudes of the first, second, and third nonzero peaks of spH ΔF histograms for WT (black) and DKO (gray) boutons. The amplitudes were obtained from the best-fit model (error bars represent SD). (*B*) Histogram of amplitudes ΔF evoked by 1 AP after 2 min of prebleaching in spH-expressing DKO boutons shows "recovery" of the first nonzero peak. Superimposed is the best-fit Gaussian curve (adjusted $R^2 = 0.89$) with a unitary size of 15.0 ± 0.50 a.u. ($n > 100$ boutons from five experiments). (*C*) Bar diagram showing relative amplitudes expressed as the ratio of the first nonzero peak to the second nonzero peak for WT (black), DKO (gray), and boutons prebleached for 2 min from DKO (blue) and WT (red) neurons (error bars represent SD). (*D*) Immunoblot of lysates from DKO, WT, spH-overexpressing DKO or WT neuronal cultures probed with anti-syb2 antibody (mouse monoclonal, 69.1). Endogenous syb2 runs at ~16 kDa, whereas overexpressed syb2 fused to pHluorin should be shifted by ~27 kDa. Thus, the single band at ~40 kDa corresponds to uncleaved spH. Note the absence of any cleaved syb2 product at ~16 kDa. The loading control used was lactate dehydrogenase (LDH) and shows nearly equal loading of the samples. (*E*) Illustration of SV fusion driven by two SNARE complexes during neuroexocytosis: assembly of two SNARE complexes with syb2 (blue) and syntaxin-1A (red) contributing one helix and SNAP-25 (green) contributing two helices. The transmembrane regions of the SNARE proteins are depicted in yellow [better seen in the version with a cut-open fusion pore (*Right*)].

thermal titration calorimetry, the free energy estimated for the assembly of individual SNARE complexes was found to be sufficient for membrane fusion (43). Thus, assembly of one SNARE complex could in theory drive fusion. Indeed, a recent study based on in vitro Förster resonance energy transfer experiments indicates that liposomes bearing only a single SNARE molecule are still capable of fusion with other liposomes or purified SVs (13). Why in vivo more SNARE complexes are needed than in vitro remains to be elucidated. One reason might be the different timescales on which SV fusion and in vitro fusion proceed: Whereas AP-triggered SV fusion in our experiments is completed within milliseconds, in vitro fusion takes seconds, indicating another very slow rate-limiting step upstream of SNARE complex formation in vitro. A trivial reason might be that syb2 is trafficked to the synapse and hence SVs as dimers (44). In this case, however, we would expect suppression not only of the first but also of the third peak in the amplitude histogram of spH expressing DKO neurons, which we did not observe. Finally, it needs to be borne in mind that in the reconstitution experiments SNAREs were fully active and not complexed to any of the control proteins such as synaptotagmin, Munc18, or complexin, whose binding in turn lowers the total energy that becomes available for fusion during SNARE assembly. In conclusion, our finding that two syb2 molecules and likely two SNARE complexes are sufficient and necessary for SV priming and fast Ca^{2+}-triggered exocytosis fundamentally revises our understanding of SNARE-mediated fusion pore formation and membrane fusion.

Materials and Methods

Cell Culture and Transfection. Primary cultures of hippocampal neurons were prepared from newborn (P0) C57BL/6 mice as previously described (23). The syb2/ceb2 DKO mice were obtained from Dieter Bruns (University of Saarland, Homburg, Germany). Because the syb2/ceb2 DKO mice are postnatal lethal (30, 31), hippocampi from embryonic day (E)18 pups were used. As a WT control we used E18 pups from separately bred C57BL/6 mice. Neurons were grown on an astrocyte feeder layer and transfected at 3 d in vitro (DIV) by a modified calcium phosphate transfection procedure (23). For details on the pHluorin–fusion constructs, lentiviral transduction, and immunoblotting see *SI Materials and Methods*.

Optical Imaging. Microscopy was performed at 14–21 DIV. Coverslips were placed in a perfusion chamber (~500 μL vol) containing a modified Tyrode's solution (140 mM NaCl, 5 mM KCl, 2 mM $CaCl_2$, 2 mM $MgCl_2$, 30 mM glucose, 10 mM Hepes, pH 7.4; ~330 mOsm). APs were elicited by electric field stimulation with 1-ms pulses of 50 mA generated by a constant current stimulus isolator (WPI A 385; World Precision Instruments) between plati-

num–iridium electrodes (distance ~1 cm) in the presence of 6-cyano-7-nitroquinoxaline-2,3-dione (CNQX, 10 μM; Tocris Bioscience) and D-amino-5-phosphonovaleric acid (D,L-APV, 50 μM; Tocris Bioscience) to prevent recurrent activity. Folimycin (Calbiochem) was used at a concentration of 65 nM. Ammonium chloride solution (pH 7.4) was prepared by substituting 50 mM NaCl in normal saline with NH_4Cl, whereas the remaining constituents were unchanged.

Experiments were conducted at room temperature on an inverted Nikon TE2000 microscope equipped with a 100×/1.45 NA oil immersion objective (Nikon). The pHluorin fusion constructs were excited at 488 nm by a mechanically shuttered Argon laser whose beam was slightly defocused at the back focal plane to fill the field of view (17 mW at the back-focal plane). Images (128 × 128 pixels) were acquired with a back-illuminated EMCCD camera (DV-860 camera; Andor Technology) at a 100-Hz frame rate using 9.6 ms exposure time during short 0.5-s periods of constant laser illumination to minimize photobleaching. Please note the optical settings for bulk experiments (Fig. 2 *A*–*G* and Fig. S2) were different and are described in *SI Materials and Methods*.

Single-Molecule pHluorin Experiments. The pHluorin expression construct was designed and generated together with Entelechon. The purified pHluorin protein was immobilized in a polyacrylamide gel (26). Experiments were performed using the same laser intensity and camera settings as in the neuronal experiments. Images were acquired at 15 Hz (9.6-ms exposure). Square regions of interest (ROIs) (1 × 1 μm) were overlaid on fluorescence spots and mean intensities were plotted. Single-molecule fluorescence amplitude was calculated by subtracting an average of 5–10 frames before and after the bleaching step. Extrapolating from the measured photobleaching time constants at pH 7.4 and 9 (Fig. 1*G*), we estimated that 50 s surface fluorescence prebleaching results in up to 20% bleaching of the vesicular fraction of spH resident at pH 5.5. Next we plotted the normalized amplitude of the first nonzero peak (normalized to failure peak) against the fraction of vesicular spH bleached as estimated above (Fig. S7). The two data points denote the two prebleaching durations used: 50 s and 2 min in Fig. 3*A* and Fig. 4*B*, respectively. The *y*-intercept yields the amplitude of the one-molecule peak for zero prebleaching.

Image and Data Analysis. Data were acquired using the Andor IQ software suite (Andor Technology). Quantitative analysis was performed with MetaMorph 6.0 (Molecular Devices) and with self-written macros in Igor Pro-6.03A (WaveMetrics). To avoid the bias introduced by manual selection of functional boutons, an automated detection algorithm was used to localize the active boutons. The ΔF histograms of single AP responses from spH, syp-pHl, and vGlut-pHl transfected boutons were fit to a multimodal Gaussian distribution constrained by the quantal size and coefficient of variation on the basis of previously described procedures (22, 24, 25). The single AP ΔF distributions in Fig. 3*B* did not alter in overall shape with increase in sample size as revealed by bootstrap analysis (Fig. S8). As expected from Poisson statistics, the peaks of the ΔF distributions display a slight increase in width with increasing mean amplitude (Fig. S9). For details on detection of functional boutons and data fitting, see *SI Materials and Methods*.

ACKNOWLEDGMENTS. We thank D. Bruns for providing us syb2/ceb2 DKO mice; E. Neher for support, advice, and critical reading of our manuscript; Y. Hua and A. Woehler for help with analysis; C. S. Thiel for purification of the pHluorin protein; and I. Herfort and M. Pilot for technical assistance. We thank H. Sebesse and C. P. Adam for the illustration in Fig. 4*E*. This work was supported by the Deutsche Forschungsgemeinschaft [SFB 523 and Kl 1334/1-1 (to J.K.)]. R.S. is supported by a stipend from the International Max Planck Research School in Neurosciences at the University of Göttingen.

1. Jahn R, Scheller RH (2006) SNAREs—engines for membrane fusion. *Nat Rev Mol Cell Biol* 7:631–643.
2. Söllner T, Bennett MK, Whiteheart SW, Scheller RH, Rothman JE (1993) A protein assembly-disassembly pathway in vitro that may correspond to sequential steps of synaptic vesicle docking, activation, and fusion. *Cell* 75:409–418.
3. Söllner T, et al. (1993) SNAP receptors implicated in vesicle targeting and fusion. *Nature* 362:318–324.
4. Hanson PI, Roth R, Morisaki H, Jahn R, Heuser JE (1997) Structure and conformational changes in NSF and its membrane receptor complexes visualized by quick-freeze/deep-etch electron microscopy. *Cell* 90:523–535.
5. Weber T, et al. (1998) SNAREpins: Minimal machinery for membrane fusion. *Cell* 92: 759–772.
6. Hu C, et al. (2003) Fusion of cells by flipped SNAREs. *Science* 300:1745–1749.
7. Lin RC, Scheller RH (1997) Structural organization of the synaptic exocytosis core complex. *Neuron* 19:1087–1094.
8. Montecucco C, Schiavo G, Pantano S (2005) SNARE complexes and neuroexocytosis: How many, how close? *Trends Biochem Sci* 30:367–372.
9. Tokumaru H, et al. (2001) SNARE complex oligomerization by synaphin/complexin is essential for synaptic vesicle exocytosis. *Cell* 104:421–432.
10. Bowen ME, Weninger K, Brunger AT, Chu S (2004) Single molecule observation of liposome-bilayer fusion thermally induced by soluble N-ethyl maleimide sensitive-factor attachment protein receptors (SNAREs). *Biophys J* 87:3569–3584.
11. Mohrmann R, de Wit H, Verhage M, Neher E, Sørensen JB (2010) Fast vesicle fusion in living cells requires at least three SNARE complexes. *Science* 330:502–505.
12. Karatekin E, et al. (2010) A fast, single-vesicle fusion assay mimics physiological SNARE requirements. *Proc Natl Acad Sci USA* 107:3517–3521.
13. van den Bogaart G, et al. (2010) One SNARE complex is sufficient for membrane fusion. *Nat Struct Mol Biol* 17:358–364.
14. Domanska MK, Kiessling V, Stein A, Fasshauer D, Tamm LK (2009) Single vesicle millisecond fusion kinetics reveals number of SNARE complexes optimal for fast SNARE-mediated membrane fusion. *J Biol Chem* 284:32158–32166.
15. Li F, et al. (2007) Energetics and dynamics of SNAREpin folding across lipid bilayers. *Nat Struct Mol Biol* 14:890–896.
16. Han X, Wang CT, Bai J, Chapman ER, Jackson MB (2004) Transmembrane segments of syntaxin line the fusion pore of Ca2+-triggered exocytosis. *Science* 304:289–292.
17. Hua Y, Scheller RH (2001) Three SNARE complexes cooperate to mediate membrane fusion. *Proc Natl Acad Sci USA* 98:8065–8070.
18. Keller JE, Cai F, Neale EA (2004) Uptake of botulinum neurotoxin into cultured neurons. *Biochemistry* 43:526–532.
19. Miesenböck G, De Angelis DA, Rothman JE (1998) Visualizing secretion and synaptic transmission with pH-sensitive green fluorescent proteins. *Nature* 394:192–195.
20. Balaji J, Ryan TA (2007) Single-vesicle imaging reveals that synaptic vesicle exocytosis and endocytosis are coupled by a single stochastic mode. *Proc Natl Acad Sci USA* 104: 20576–20581.
21. Granseth B, Odermatt B, Royle SJ, Lagnado L (2006) Clathrin-mediated endocytosis is the dominant mechanism of vesicle retrieval at hippocampal synapses. *Neuron* 51: 773–786.
22. Gandhi SP, Stevens CF (2003) Three modes of synaptic vesicular recycling revealed by single-vesicle imaging. *Nature* 423:607–613.
23. Wienisch M, Klingauf J (2006) Vesicular proteins exocytosed and subsequently retrieved by compensatory endocytosis are nonidentical. *Nat Neurosci* 9:1019–1027.
24. Lemke EA, Klingauf J (2005) Single synaptic vesicle tracking in individual hippocampal boutons at rest and during synaptic activity. *J Neurosci* 25:11034–11044.
25. Murthy VN, Stevens CF (1998) Synaptic vesicles retain their identity through the endocytic cycle. *Nature* 392:497–501.
26. Kubitscheck U, Kückmann O, Kues T, Peters R (2000) Imaging and tracking of single GFP molecules in solution. *Biophys J* 78:2170–2179.
27. Sankaranarayanan S, De Angelis D, Rothman JE, Ryan TA (2000) The use of pHluorins for optical measurements of presynaptic activity. *Biophys J* 79:2199–2208.
28. Fernández-Alfonso T, Kwan R, Ryan TA (2006) Synaptic vesicles interchange their membrane proteins with a large surface reservoir during recycling. *Neuron* 51: 179–186.
29. Takamori S, et al. (2006) Molecular anatomy of a trafficking organelle. *Cell* 127: 831–846.
30. Borisovska M, et al. (2005) v-SNAREs control exocytosis of vesicles from priming to fusion. *EMBO J* 24:2114–2126.
31. Schoch S, et al. (2001) SNARE function analyzed in synaptobrevin/VAMP knockout mice. *Science* 294:1117–1122.
32. Deák F, Shin OH, Kavalali ET, Südhof TC (2006) Structural determinants of synaptobrevin 2 function in synaptic vesicle fusion. *J Neurosci* 26:6668–6676.
33. Guzman RE, Schwarz YN, Rettig J, Bruns D (2010) SNARE force synchronizes synaptic vesicle fusion and controls the kinetics of quantal synaptic transmission. *J Neurosci* 30: 10272–10281.
34. Sankaranarayanan S, Ryan TA (2001) Calcium accelerates endocytosis of vSNAREs at hippocampal synapses. *Nat Neurosci* 4:129–136.
35. Knowles MK, et al. (2010) Single secretory granules of live cells recruit syntaxin-1 and synaptosomal associated protein 25 (SNAP-25) in large copy numbers. *Proc Natl Acad Sci USA* 107:20810–20815.
36. Ulbrich MH, Isacoff EY (2007) Subunit counting in membrane-bound proteins. *Nat Methods* 4:319–321.
37. Voets T, et al. (2001) Munc18-1 promotes large dense-core vesicle docking. *Neuron* 31: 581–591.
38. de Wit H, Cornelisse LN, Toonen RF, Verhage M (2006) Docking of secretory vesicles is syntaxin dependent. *PLoS ONE* 1:e126.
39. de Wit H, et al. (2009) Synaptotagmin-1 docks secretory vesicles to syntaxin-1/SNAP-25 acceptor complexes. *Cell* 138:935–946.
40. Jackson MB, Chapman ER (2008) The fusion pores of Ca2+ -triggered exocytosis. *Nat Struct Mol Biol* 15:684–689.
41. Kozlovsky Y, Kozlov MM (2002) Stalk model of membrane fusion: Solution of energy crisis. *Biophys J* 82:882–895.
42. Cohen FS, Melikyan GB (2004) The energetics of membrane fusion from binding, through hemifusion, pore formation, and pore enlargement. *J Membr Biol* 199:1–14.
43. Wiederhold K, Fasshauer D (2009) Is assembly of the SNARE complex enough to fuel membrane fusion? *J Biol Chem* 284:13143–13152.
44. Fdez E, et al. (2008) A role for soluble N-ethylmaleimide-sensitive factor attachment protein receptor complex dimerization during neurosecretion. *Mol Biol Cell* 19: 3379–3389.